Three-Dimensional Carbon Nanotube Scaffolds as Particulate Filters and Catalyst Support Membranes

Niina Halonen,[†] Aatto Rautio,[†] Anne-Riikka Leino,[†] Teemu Kyllönen,[†] Géza Tóth,[†] Jyrki Lappalainen,[†] Krisztián Kordás,[†] Mika Huuhtanen,[‡] Riitta L. Keiski,[‡] András Sápi,[§] Mária Szabó,[§] Ákos Kukovecz,[§] Zoltán Kónya,[§] Imre Kiricsi,[§] Pulickel M. Ajayan,[⊥] and Robert Vajtai[⊥,*]

[†]Microelectronics and Materials Physics Laboratories, and EMPART Research Group of Infotech Oulu, Department of Electrical and Information Engineering, University of Oulu; P.O. Box 4500, FIN-90014 University of Oulu, Finland, [‡]Mass and Heat Transfer Process Laboratory, Department of Process and Environmental Engineering, University of Oulu, P.O. Box 4300, FIN-90014 University of Oulu, Finland, [§]Department of Applied and Environmental Chemistry, University of Szeged, Rerrich B. tér 1, H-6720 Szeged, Hungary, and [⊥]Department of Mechanical Engineering and Materials Science, Rice University, Houston, Texas 77005

ABSTRACT Three-dimensional carbon nanotube scaffolds created using micromachined Si/SiO_2 templates are used as nanoparticulate filters and support membranes for gas-phase heterogeneous catalysis. The filtering efficiency of better than 99% is shown for the scaffolds in filtering submicrometer particles from air. In the hydrogenation of propene to propane reaction low activation energy of $E_a \sim 27.8 \pm 0.6$ kJ · mol^{-1}, a considerably high turnover rate of ~1.1 molecules · Pd site^{-1} · s^{-1} and durable activity for the reaction are observed with Pd decorated membranes. It is demonstrated that appropriate engineering of macroscopic-ordered nanotube architectures can lead to multifunctional applications.

KEYWORDS: carbon nanotubes · catalyst support · submicrometer filtering · air filter · propene

Organizing nanomaterials into macroscopic systems is the bottleneck in nanotechnology today, as the engineering of these structures often compromise their intrinsic properties. On the other hand, applications of nanomaterial aggregates in areas such as catalysis and filtration have shown superior performance.[1,2] Macroscopic assemblies of robust aligned carbon nanotube (CNT) films used as nanoelectromechanical systems and nanoelectronic devices,[3] brush-type electrodes,[4] multifunctional nanobrushes,[5] and chip cooling elements,[6] *etc.* have demonstrated the utility of large blocks and microscopic arrays of ordered nanotubes. The CNT structures can be synthesized directly by catalytic chemical vapor-phase deposition methods on planar as well as three-dimensional growth templates with well-defined geometries.[7] Here we present a simple but efficient route to organize aligned carbon nanotubes into macroscopic membranes which can be used as particulate filters and catalyst templates. We demonstrate the performance of these filters by showing the removal of more than 99% of the particulates with submicrometer diameter. We show that a similar scaffold system decorated with Pd nanoparticles also serves as excellent catalyst support in the hydrogenation of propene to propane.

RESULTS

Chemical vapor deposition (CVD) on the micromachined Si/SiO_2 wafers produces well-aligned nanotubes perpendicular to the SiO_2 surface both on the upper/lower facets of the template and also on the cylindrical surface of the laser-ablated holes (Figure 1). The holes become gradually filled in as the CVD process evolves in time, and after ~30 min synthesis, no macroscopic or microscopic pinholes can be observed. In the case of longer deposition, the film gets densified and then the nanotubes bend and continue to grow parallel to the walls of the holes (instead of the perpendicular direction; see Figure 1).

The gas permeability of membranes shows significant dependence on the CNT length, structure, and density in the scaffold (Figure 2a). When short growth time (see Materials and Methods) is used, the pinholes in the membranes enable strong flow through of gases. Testing of membrane grown for the longest time in particulate air filtering shows higher than 99% filtering efficiency for particles having a size of 0.3 μm, which is considerably better than that obtained for the material used as the household HEPA filter (Figure 2b).

To demonstrate the feasibility of the membranes in catalysis, the nanotubes were first decorated with Pd nanoparticles

*Address correspondence to Robert.Vajtai@rice.edu.

Received for review January 25, 2010 and accepted March 24, 2010.

Published online April 6, 2010. 10.1021/nn100150x

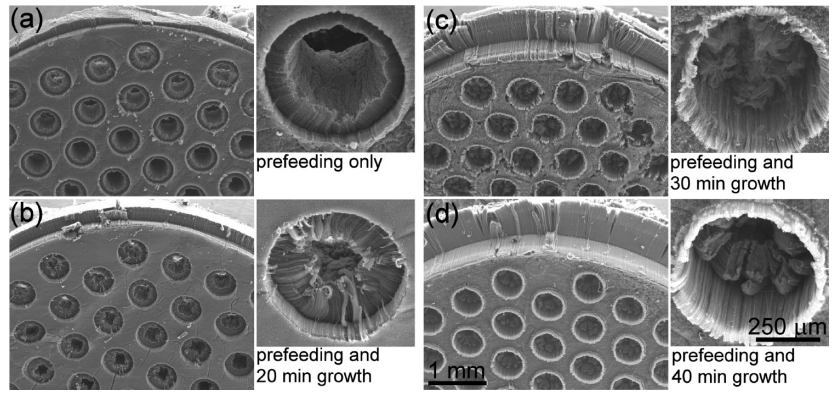

Figure 1. FESEM images of various carbon nanotube membranes grown on microstructured and oxidized Si chips: synthesis times of (a) 0, (b) 20, (c) 30, and (d) 40 min were applied after the precursor prefeeding step.

and then applied as a membrane catalyst for reducing propene to propane with H_2. For Pd deposition on CNTs two different approaches were used: in the first one, the membranes were impregnated with Pd−acetate and reduced/activated in H_2 flow at 500 °C; while in the other process, the impregnated membranes were calcined in air at 380 °C before the reduction step. The Pd nanoparticles show narrow size distribution with a mean diameter of 3.4 ± 1.5 and 5.4 ± 3.6 nm for reduced only and for calcined and reduced samples, respectively (Figure 3). The calculation of the turnover rates and dispersion was based on the diameters of the Pd nanoparticles determined from TEM images (Figure 3) and assuming that each Pd atom at the monolayer surface is an active site.[8] The dispersion of catalyst was ~0.24 and ~0.11 for the reduced and calcined-reduced samples, respectively.

The activated catalyst membranes showed excellent and durable activity in the hydrogenation of propene to propane in the case of the three samples filled with the longest carbon nanotubes. The turnover rate was ~1.1 molecules · Pd site^{-1} · s^{-1} in the $t > 120$ °C temperature range (Figure 4b) even after three consecutive experimental tests. The short CNT membranes grown only by prefeeding showed a maximum ~0.7 molecules · Pd site^{-1} · s^{-1}, because some molecules can pass through of the central hole of the membrane. The conversion was found to be weakly dependent on the method of catalyst preparation. Despite the higher dispersion, the reduced catalyst showed only slightly better maximum conversion values than those calcined before activation which can be attributed to the partial poisoning of metallic active sites.

Arrhenius behavior (Figure 4c) shows the three different catalytic reaction regimes typical for porous solid catalysts.[9] After a number of repeated heating and cooling cycles the catalyst was tested in an aging test at a relatively high temperature (156.1 ± 2.4 °C) and showed no sign of deactivation until after a 2 h time-on-stream run (Figure 4d). Furthermore, when the catalyst is removed from the reactor and stored in ambient atmosphere and reduced again, the same activity could be recovered as before. An increase of the catalyst size (Figure 4e) due to coarsening upon usage was well within the error of the measurements (Supporting Information, Figure S1).

DISCUSSION

In this work we show a simple and facile route to fabricate carbon nanotube membranes on microstructured Si/SiO_2 chips for particulate air filtering and catalyst support applications. The permeability of membranes is adjusted by the growth time applied in the catalytic CVD of carbon nanotubes. The intrinsic

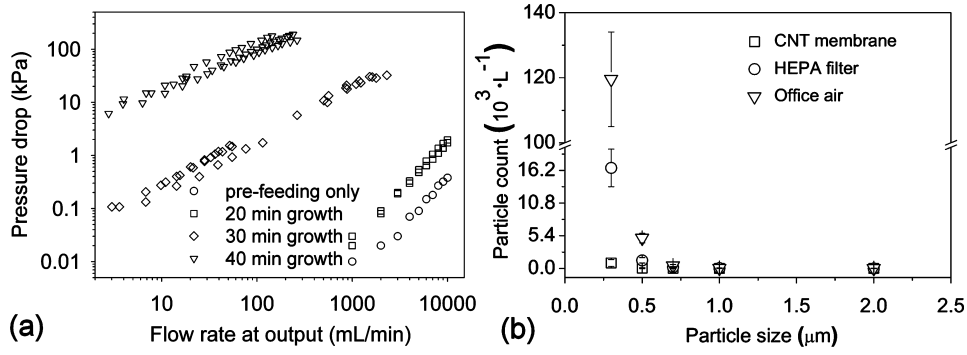

Figure 2. (a) Pressure drop *vs* flow rate of nanotube membranes. Samples with longer growth time show decreased permeability due to the tortuous CNT films and closed up macroscopic holes (in each case, 2 mL precursor prefeeding has been applied before growth). (b) Concentration of the particulates with a diameter of 0.3−2 μm in office air before and after filtering through the CNT membrane grown for 40 min and a sheet of commercial household HEPA filter of ~200 μm thickness.

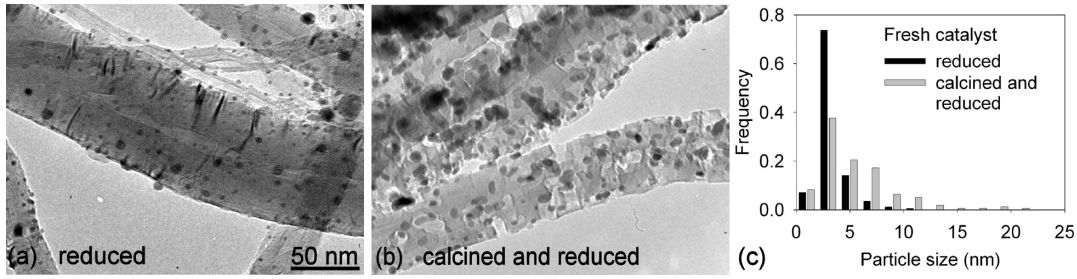

Figure 3. TEM images of carbon nanotubes decorated with Pd nanoparticles: (a) Pd−acetate impregnated on CNTs is reduced in H_2 flow at 500 °C resulting in Pd nanoparticles of 3.4 ± 1.5 nm diameters; (b) impregnated sample calcined in air at 380 °C before the reduction step having average catalyst size of 5.4 ± 3.6 nm. (c) Size of the Pd nanoparticles in the fresh samples.

permeability (μ) of different membranes can be estimated by applying Darcy's equation, $\Delta p = (\eta LQ)/(A\mu)$, where a constant pressure gradient is assumed in the membranes, as $\mu = (\eta LQ)/(A\Delta p)$, where $\eta = 2 \times 10^{-5}$ Pa · s is the dynamic viscosity of Ar, $L = 5 \times 10^{-4}$ m is the thickness of the membrane, $A = 16.7 \times 10^{-6}$ m^2 is the total cross section of gas flow, Q is the gas flow rate, and Δp is the pressure drop on the membranes (Table 1).

Samples of short growth time give the highest permeabilities due to the strong through flow in the only partially filled microscopic flow channels. The permeability values of the other samples which were grown using longer synthesis times show reasonable agreement with the values measured on other porous carbonaceous media[10] similar in densities to our nanotube films[6] (~150−200 kg · m^{-3} measured for noncompressed planar aligned films). For instance, the intrinsic gas permeability of highly porous graphite matrices having densities between $\rho = 20-200$ kg · m^{-3} was measured to be in the range from 10^{-12} to 10^{-15} m^2.[11] Similar results, 2.5×10^{-14} to 10^{-15} m^2 were obtained for compressed exfoliated graphite (ρ = 100−190 kg · m^{-3}).[12] The large difference (~50-times) of the permeability for the samples grown for 40 min compared to 30 min can be explained on the basis of the limited percolation of the pores through the film.[10]

The nanotube membranes with lower permeability showed ~99% filtering efficiency in the case of

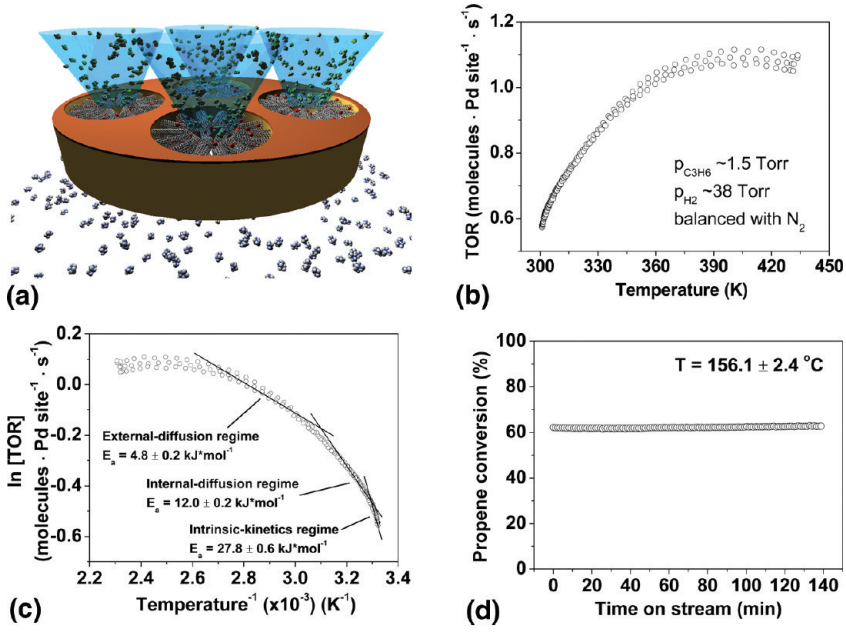

(e)

	Fresh catalyst size (nm)	Spent catalyst size (nm)
Reduced	3.4 ± 1.5	3.0 ± 1.3
Calcined and reduced	5.4 ± 3.6	6.1 ± 3.4

Figure 4. (a) Schematic view of the gas flow during catalyst activity tests on a membrane. (b) Turnover rates of propene hydrogenation to propane in the temperature range from 27 to 160 °C. Results from three consecutive measurements are in good agreement. (c) Corresponding Arrhenius type diagram shows the three different catalytic reaction regimes typical for porous solid catalysts. The intrinsic-kinetics regime is identified with apparent an activation energy of 27.8 ± 0.6 kJ · mol^{-1}. (d) Aging test of catalyst shows no deactivation after a 2 h time on stream. (e) Catalyst size determined from TEM analysis (in each case, count >160 particles).

TABLE 1. Intrinsic Permeabilities of CNT Membranes Measured in Ar Flow at 23°C

membrane	growth process	$Q/\Delta p$ ($m^3\ s^{-1}\ Pa^{-1}$)	μ (m^2)
1	prefeeding only	$(3.1 \pm 1.1) \times 10^{-8}$	$(1.88 \pm 0.68) \times 10^{-11}$
2	prefeeding and 20 min growth	$(1.7 \pm 0.1) \times 10^{-8}$	$(9.9 \pm 0.78) \times 10^{-12}$
3	prefeeding and 30 min growth	$(9.3 \pm 0.3) \times 10^{-10}$	$(5.58 \pm 0.18) \times 10^{-13}$
4	prefeeding and 40 min growth	$(2.0 \pm 0.1) \times 10^{-11}$	$(1.20 \pm 0.06) \times 10^{-14}$

particulates of submicrometer diameter. The very efficient filtering of submicrometer-sized particles through the CNT membranes is attributed to the high density packing of the nanotubes (Figure 1d) with an accompanying microporous and mesoporous structure having typical pore size on the nanometer scale (Supporting Information Figure S2) which is 3 orders of magnitude smaller than the pores of the used HEPA filter (Supporting Information Figure S3).

Membranes with higher permeability decorated with Pd nanoparticles proved to be excellent catalysts in the hydrogenation of propene to propane either as prepared or calcined. A significant difference among the obtained catalysts is the partially consumed nanotube support of calcined samples—as the catalyst nanoparticles drill nanosized holes and cavities in the walls of CNTs (Figure 3b). In the course of decomposition in air, Pd−acetate forms also PdO besides metallic Pd (Supporting Information Figure S4).[13] As the oxide phase is known to be highly reactive,[14−16] the localized catalytic oxidation of carbon is indeed possible at 380 °C in air.

Analyzing the Arrhenius plots we can consider three different catalytic reaction regimes which are typical for porous solid catalysts.[9] At low temperatures (27−31 °C) in the intrinsic-kinetics regime, the rate of the reaction is so low that the diffusion flux is insignificant, and intrinsic reaction kinetics can be assumed with an apparent activation energy of $27.8 \pm 0.6\ kJ \cdot mol^{-1}$ (approximately 290 meV per molecule). This value is slightly lower than those measured on Pt catalyst ($E_a \approx$ 35.1−58.5 $kJ \cdot mol^{-1}$) supported on various oxides[16−18] and close to $35 \pm 1\ kJ \cdot mol^{-1}$ found for Pd catalyst used in ethylene hydrogenation.[19] With increased temperature, in the internal diffusion regime (31−41 °C) the pore diffusion becomes significant compared to the increased reaction rate. In this regime the observed activation energy is $12.0 \pm 0.2\ kJ \cdot mol^{-1}$, which is approximately one-half of the intrinsic value, which is in good agreement with calculations described for this regime.[9] At higher temperatures (external diffusion regime) the rate-limiting step is the mass transfer from ambient fluid to the surface observed in apparent activation energy with a value of $4.8 \pm 0.2\ kJ \cdot mol^{-1}$ occurred at bulk diffusion characteristics of gases in porous solid catalysts.[9] The deviation at higher temperatures (>105 °C) may be attributed to changes in kinetics and appearance of other reactions such as dehydrogenation of propane (C_3H_8) to propene (C_3H_6) or propene to propyne (C_3H_4).

The high sintering resistance of Pd nanoparticles upon prolonged exposure to elevated temperature is most likely related to the stabilization effect exercised by the ordered porous structure of the radial carbon nanotube network. A similar phenomenon was reported on the stabilization effect of SBA-15 mesopores on supported 2−6 nm Pd nanopartices calcined in air at 550 °C.[20] Similar high sintering resistance—caused by the carbonaceous surroundings and pore entrapment—of Pt nanoparticles enclosed in microporous hollow carbon shells was demonstrated up to 800 °C.[21]

MATERIALS AND METHODS

Template Fabrication. We use silicon chips (thickness of ~500 μm) that are laser cut to small discs (~8.5 mm in diameter) and drilled through to form cylindrical holes (~500 μm diameter) in a hexagonal arrangement (with a center-to-center spacing of 1 mm). For microstructuring the Si wafers, a Nd:YVO_4 pulsed laser has been used. The laser parameters are as follows: pulse duration of 20 ns, focal spot size of ~15 μm, repetition rate of 20 kHz, average power of 3.2 W and scan rate of 50 mm/s. The microstructured wafers are cleaned in KOH solution (1 M, 23 °C, 2−3 min) to remove Si debris formed in the laser ablation process, then oxidized in air at 1000 °C for 12 h to generate a thin diffusion barrier surface oxide layer suitable for growing carbon nanotubes by catalytic chemical vapor deposition.

Catalytic Chemical Vapor Deposition of Multiwalled Carbon Nanotubes. Growth of carbon nanotubes has been achieved in a horizontal tube reactor from xylene/ferrocene precursor as described elsewhere.[4,6,7] In brief, the reactor is pumped to a base pressure below 0.5 Torr and purged with argon. The argon flow rate is then set to ~40 $mL \cdot min^{-1}$ and the reactor is heated to 770−785 °C. A nominal 2 mL aliquot of precursor solution (20 g of ferrocene dissolved in 1000 mL of xylene) is injected into an evaporator column preheated to 185 °C, and then the vapor is introduced into the reactor with the preset flow rate of argon gas. After the parameters were stabilized, the precursor flow rate is adjusted to 0.1 $mL \cdot min^{-1}$ and maintained until the end of the process (20−40 min).

Gas Permeability Measurements. The nanotube membranes were mounted in a silicon rubber tube which provided good sealing along the perimeter. The flow rate of Ar gas was measured using different flow meters measuring from 5 $mL \cdot min^{-1}$ up to 10 $L \cdot min^{-1}$. The pressure drop on the membranes was measured using a regulator gauge (AGA, R40/A1 GB from 30 kPa up to 200 kPa), a piezo transducer (HPS series 902 from 2 to 30 kPa), and a manometer (0.01−2 kPa).

Testing in Particulate Air Filtering. Ambient air with a flow rate of 30 $mL \cdot min^{-1}$ was flowed through the as-prepared membranes and a sheet of a household HEPA air filter (Ideale; class H10) of ~200 μm thickness tightened to a silicon tube as reference material. The concentration of particles with diameter of 0.3−2

μm in outlet gas was monitored by a Lighthouse hand-held 3016 IAQ airborne laser particle counter.

Specific Surface Area Determination of the Nanotubes. N_2 adsorption isotherms were measured at 77 K using a Quantachrome NOVA 2200 facility. The specific surface area (A_{BET}) was calculated from the 0.1−0.3 p/p_0 region of the adsorption isotherm using the Brunauer−Emmett−Teller (BET) method. The pore diameter (d_{BJH}) was calculated by the Barret−Joyner−Halenda (BJH) method from the adsorption isotherm in order to avoid an artifact due to the tensile strength effect.[22]

Catalyst Deposition on the CNT Membranes. The catalyst particles are deposited by wetness impregnation widely used for powder support samples.[23−26] Our process is as follows: $Pd(OAc)_2$ dissolved in toluene (9.8 mg · mL^{-1}) is drop cast on the nanotube samples until the *ca.* 30−35 wt % Pd load is reached. The "reduced catalyst" samples are made by heating the membranes from room temperature (RT) to 500 °C in 5% H_2/N_2 flow with a rate of 5 °C · min^{-1}, then keeping the membranes at 500 °C for 5 min and finally cooling back to RT. The "calcined-reduced catalysts" are prepared by drying in air at 105 °C for 30 min followed by calcination at 185 °C for 1 h and then at 380 °C for 1 h. Then the same reduction procedure is carried out as described above for the "reduced catalyst".

Catalyst Characterization. X-ray diffraction experiments were performed using Cu Kα radiation (Siemens D5000 diffractometer). Electron microphotographs of the samples were taken by a LEO 912 OMEGA energy-filtered transmission electron microscope using 120 kV acceleration voltage. Histograms of particle size distribution were obtained by counting at least 160 particles on the micrographs of 250 k magnification for each sample.

Catalyst Activity and Reliability Tests. In the activity experiments, the catalyst samples were fixed tightly in a quartz reactor of 9 mm inner diameter. The temperature at the membranes was measured with a thermocouple being placed in the plane of the membrane. The inlet gas composition (~1.5 Torr propene, ~38 Torr H_2 balanced with N_2 on ambient pressure), and flow rates (1000 mL · min^{-1}) were set using mass-flow controllers. The outlet gas composition (propane and propene) was measured by an FT-IR (Gasmet) gas analyzer. Basically two different types of experiments were carried out to collect information on the catalytic behavior of the membranes. In the first, the reactor temperature was ramped up from 25 to 160 °C then cooled back to ~25 °C with a rate of 10 °C · min^{-1}. This was repeated at least three times to study the repeatability of experiments and possible deactivation of the catalyst upon temperature cycling. In the other experiment, the cycled catalyst samples were left in the reactor and the temperature was set to ~155 °C, while the propene to propane conversion was monitored as a function of time (time-on-stream measurement), again to study catalyst deactivation.

Acknowledgment. The authors are grateful for financial support received from TEKES (projects: 52423 and 52433) and Academy of Finland (projects: 120853, 124357, 128626, 128908) K. Kordas is grateful for the support (research fellow post and incentive funding) received from the Academy of Finland. N. Halonen acknowledges her post granted by the National Graduate School in Nanosciences. Á. Kukovecz acknowledges support from the OTKA NNF 78920 project. The authors are grateful for the technical support of the Micro and Nanotechnology Centre, University of Oulu.

Supporting Information Available: Results of characterization of the catalyst materials as well as the HEPA filters used as reference. This material is available free of charge *via* the Internet at http://pubs.acs.org.

REFERENCES AND NOTES

1. Gellman, A. J.; Shukla, N. Nanocatalysis: More than Speed. *Nat. Mater.* **2009**, *8*, 87–88.
2. Ahn, Y. C.; Park, S. K.; Kim, G. T.; Hwang, Y. J.; Lee, C. G.; Shin, H. S.; Lee, J. K. Development of High Efficiency Nanofilter Made of Nanofibers. *Curr. Appl. Phys.* **2006**, *6*, 1030–1035.
3. Sazonova, V.; Yaish, Y.; Ustunel, H.; Roundy, D.; Arias, T. A.; McEuen, P. L. A Tunable Carbon Nanotube Electromechanical Oscillator. *Nature* **2004**, *431*, 284–287.
4. Toth, G.; Mäklin, J.; Halonen, N.; Palosaari, J.; Juuti, J.; Jantunen, H.; Kordas, K.; Sawyer, W. G.; Vajtai, R.; Ajayan, P. M. Carbon-Nanotube-Based Electrical Brush Contacts. *Adv. Mater.* **2009**, *21*, 2054–2058.
5. Cao, A. Y.; Veedu, V. P.; Li, X. S.; Yao, Z. L.; Ghasemi-Nejhad, M. N.; Ajayan, P. M. Multifunctional Brushes Made from Carbon Nanotube. *Nat. Mater.* **2005**, *4*, 540–545.
6. Kordas, K.; Toth, G.; Moilanen, P.; Kumpumäki, M.; Vähäkangas, J.; Uusimäki, A.; Vajtai, R.; Ajayan, P. M. Chip Cooling with Integrated Carbon Nanotube Microfin Architectures. *Appl. Phys. Lett.* **2007**, *90*, 123105.
7. Halonen, N.; Kordas, K.; Toth, G.; Mustonen, T.; Mäklin, J.; Vähäkangas, J.; Ajayan, P. M.; Vajtai, R. Controlled CCVD Synthesis of Robust Multiwalled Carbon Natotube Films. *J. Phys. Chem. C* **2008**, *112*, 6723–6728.
8. First, from the diameter of nanoparticles we calculate the corresponding volumes and surface areas assuming a spherical shape, then take their mean to get $\langle V\rangle$ and $\langle A\rangle$. The average number of Pd atoms in the bulk $\langle N\rangle_V^{Pd}$ and on the surface $\langle N\rangle_A^{Pd}$ are obtained as $\langle N\rangle_V^{Pd} = \langle V\rangle(6.96 \times 10^{22}$ atom/cm^3) and $\langle N\rangle_A^{Pd} = \langle A\rangle(1.37 \times 10^{15}$ atom/cm^2), respectively, where 0.386 nm is the unit cell parameter of fcc Pd. The dispersion of the catalyst is defined as $\langle N\rangle_A^{Pd}/\langle N\rangle_V^{Pd}$. The turnover rate (TOR) defined as the rate of generated molecules over the number of catalyst surface atoms is estimated as

$$\mathrm{TOR} = \frac{1\ \mathrm{L/min} \times 10^5\ \mathrm{Pa} \times 2000\ \mathrm{ppm} \times 0.62}{300\ \mathrm{K} \times 8.314\ \mathrm{J/mol{\cdot}K}} \left(\frac{0.79\ \mathrm{mg} \times 0.11}{106.4\ \mathrm{g/mol}}\right)^{-1} \approx 1.1\ \mathrm{s}^{-1}$$

.
9. Satterfield, C. N. *Heterogenous Catalysis in Practice*; McGraw-Hill: New York, 1980; pp 318−328.
10. Biloé, S.; Mauran, S. Gas Flow through Highly Porous Graphite Matrices. *Carbon* **2003**, *41*, 525–537.
11. Cooper, S. M.; Chuang, H. F.; Cinke, M.; Cruden, B. A.; Meyyappan, M. Gas Permeability of a Bucky Paper Membrane. *Nano Lett.* **2003**, *3*, 189–192.
12. Celzard, A.; Marêché, J. F.; Furdin, G. Modelling of Exfoliated Graphite. *Progress Mater. Sci.* **2005**, *50*, 93–179.
13. Gallagher, P. K.; Gross, M. E. The Thermal Decomposition of Palladium Acetate. *J. Therm. Anal.* **1986**, *31*, 1231–1241.
14. Lin, R.; Luo, M. F.; Xin, Q.; Sun, G. Q. The Mechanism Studies of Ethanol Oxidation on PdO Catalysts by TPRS Techniques. *Catal. Lett.* **2004**, *93*, 139–144.
15. McCarty, J. G. Kinetics of PdO Combusition Catalysis. *Catal. Today* **1995**, *26*, 283–293.
16. Kordás, K.; Toth, G.; Levoska, J.; Huuhtanen, M.; Keiski, R.; Härkönen, M.; George, T. F.; Vähäkangas, J. Room Temperature Chemical Deposition of Palladium Nanoparticles in Anodic Aluminum Oxide Templates. *Nanotechnology* **2006**, *17*, 1459–1463.
17. Cocco, G.; Campostrini, R.; Cabras, M. A.; Carturan, G. Propene Hydrogenation on Low-Temperature Reduced Pt/TiO_2. Effects of TiO_2 Phases and H_2 Treatment on Specific Catalytic Activity. *J. Mol. Catal.* **1994**, *94*, 299–310.
18. Yoo, J. W.; Hathcock, D. J.; El-Sayed, M. A. Propene Hydrogenation over Truncated Octahedral Pt Nanoparticles Supported on Alumina. *J. Catal.* **2003**, *214*, 1–7.
19. Molero, H.; Stacchiola, D.; Tysoe, W. T. The Kinetics of Ethylene Hydrogenation Catalyzed by Metallic Palladium. *Catal. Lett.* **2005**, *101*, 145–149.
20. Yuranov, I.; Moeckli, P.; Suvorova, E.; Buffat, P.; Kiwi-Minsker, L.; Renken, A. Pd/SiO_2 Catalysts: Synthesis of Pd Nanoparticles with the Controlled Size in Mesoporous Silicas. *J. Mol. Catal. A* **2003**, *192*, 239–251.
21. Ng, Y. H.; Ikeda, S.; Harada, T.; Sakata, T.; Mori, H.; Takaoka, A.; Matsumura, M. High Sintering Resistance of Platinum Nanoparticles Embedded in a Microporous Hollow Carbon

Shell Fabricated through a Photocatalytic Reaction. *Langmuir* **2008**, *24*, 6307–6312.
22. Smajda, R.; Kukovecz, A.; Konya, Z.; Kiricsi, I. Structure and Gas Permeability of Multiwall Carbon Nanotube Buckypapers. *Carbon* **2007**, *45*, 1176–1184.
23. Serp, P.; Corrias, M.; Kalck, P. Carbon Nanotubes and Nanofibers in Catalysis. *Appl. Catal., A* **2003**, *253*, 337–358.
24. Yu, R. Q.; Chen, L. W.; Liu, Q. P.; Lin, J. Y.; Tan, K. L.; Ng, S. C.; Chan, H. S. O.; Xu, G. Q.; Hor, T. S. A. Platinum Deposition on Carbon Nanotubes *via* Chemical Modification. *Chem. Mater.* **1998**, *10*, 718–722.
25. Solhy, A.; Machado, B. F.; Beausoleil, J.; Kihn, Y.; Goncalves, F.; Pereira, M. F. R.; Orfalo, J. J. M.; Fiqueiredo, J. L.; Faria, J. L.; Serp, P. MWCNT Activation and Its Influence on the Catalytic Performance of Pt/MWCNT Catalysts for Selective Hydrogenation. *Carbon* **2008**, *46*, 1194–1207.
26. Tavasoli, A.; Abbaslou, R. M. M.; Trepanier, M.; Dalai, A. K. Fischer−Tropsch Synthesis over Cobalt Catalyst Supported on Carbon Nanotubes in a Slurry Reactor. *Appl. Catal., A* **2008**, *345*, 134–142.